International Journal of GEOMATE, Nov., 2024 Vol.27, Issue 123, pp.65-74
ISSN: 2186-2982 (P), 2186-2990 (O), Japan, DOI: https://doi.org/10.21660/2024.123.4632
Geotechnique, Construction Materials and Environment

SEISMIC DAMAGE PREDICTION OF SELECTED REINFORCED CONCRETE STRUCTURES IN MARIKINA CITY USING FRAGILITY CURVE

*Justin Lorenz A. Lim[1] and Gilford B. Estores[2]

[1]School of Graduate Studies, Mapua University, Philippines
[2]School of Civil, Environmental, and Geological Engineering, Mapua University, Philippines

*Corresponding Author, Received: 12 July 2024, Revised: 08 Oct. 2024, Accepted: 09 Oct. 2024

ABSTRACT: The West Valley Fault, the source of the anticipated 7.2 magnitude earthquake or the "Big One," is said to have a return period of 500 years and has not moved since the 1600s. This study aims to predict the structural damage to be sustained by six existing reinforced concrete structures within a two-kilometer range from the fault line in Marikina City if the anticipated earthquake hits using a fragility curve. Nonlinear static pushover analysis was done to generate the idealized force-displacement curve, and then capacity spectrum conversion was performed to determine the structural damage states. Four distinct graphs are plotted in a single fragility curve; each represents a structural damage state, which is qualitatively and quantitatively defined. Due to the unpredictability of seismic motion, damage prediction is conducted separately in two different seismic directions. Given each structure's critical direction, it shows a probability ranging from 63.53% to 90.97% that it would suffer from some degree of structural damage. The structure with the highest likelihood of collapse is 21.16%, while the rest of the structures' collapse probability ranges from 1.14% to 7.17% in their critical direction. The severity of structural damage varies depending on the structure's configuration with respect to the fault line, the direction of the seismic motion, and the column dimension. A special moment frame for reinforced concrete structures is recommended since Marikina City is under Seismic Zone 4, and a minimum dimension of 300mm for all structural columns should be complied with.

Keywords: Earthquake, West Valley Fault, Damage Prediction, Fragility Curve, Reinforced Concrete Structures

1. INTRODUCTION

The so-called "Big One," an earthquake with a magnitude of 7.2, is expected to strike the National Capital Region of the Philippines. JICA, MMDA, and PHIVOLCS [1] stated that Marikina City is one of the main cities the West Valley Fault crosses. For the past 1400 years, the West Valley Fault has caused seismic activities. It has moved around every 500 years, and there has been no recorded motion since the 17th century. According to the seismic map provided by the National Structural Code of The Philippines (NSCP 2015) [2], the Philippines is mainly under Zone 4, including Marikina City, making it crucial for engineers to evaluate the population's awareness to lessen serious injuries, casualties, and damages.

Some structures in Marikina City were not compliant with the minimum dimensional requirement for columns in special moment frames, which is 300mm, as prescribed by the American Concrete Institute Committee 318 [3], so there is an urgency to predict the structural damage to selected reinforced concrete structures in case the 7.2 magnitude earthquake hits and the predicted severity of the damage could be used as a guide for the rehabilitation of the existing structures and for future construction projects. Karimzadeh et al. [4] mentioned limited methods for assessing damages due to seismic action; however, fragility curves have been studied in multiple literature reviews to predict the severity of structural damage to structures.

Alothman et al. [5] stated that fragility curves are often applied to evaluate the seismic performance of vertical structures. To further back up the use of fragility curves for predicting seismic damage on reinforced concrete structures, Ghani et al. [6] affirm that fragility curves, defined by the lognormal cumulative distribution functions, are a reliable indicator of how structures can withstand an earthquake as it shows the probability of the earthquake exceeding a particular damage state on a structure. The same can be said in the study of Vasileiadis et al. [7], which describes the fragility curve as a representation of the structure's seismic vulnerability by plotting the probabilities of exceeding different prescribed damage states as a function of intensity.

The fragility curves generated in this study are similar to those developed by Gentile et al. [8]. Both are defined as lognormal cumulative distribution functions, which plot the probability that a specific damage state would be exceeded in the vertical axis, and each fragility curve is composed of four curves, each representing the structural damage states. However, the intensity measure plotted in the horizontal axis used in this study is the spectral displacement because it would provide the foundation for obtaining the qualitative description and the

quantitative values for the structural damage states.

The six reinforced concrete structures were modeled in SAP2000, followed by conducting a nonlinear static pushover analysis that would yield the idealized force-displacement curves, which are used to perform the capacity spectrum conversion to determine the spectral displacements that would be correlated to the structural damage states. Two fragility curves were generated per structure, representing the global east-west and north-south directions. Damage prediction was conducted separately for the two seismic directions due to the unpredictability of the seismic motion. Fig. 1 shows the map that includes the orientation for the global east-west direction and the global north-south direction, along with the West Valley Fault, including Marikina City on the eastern side of the fault line.

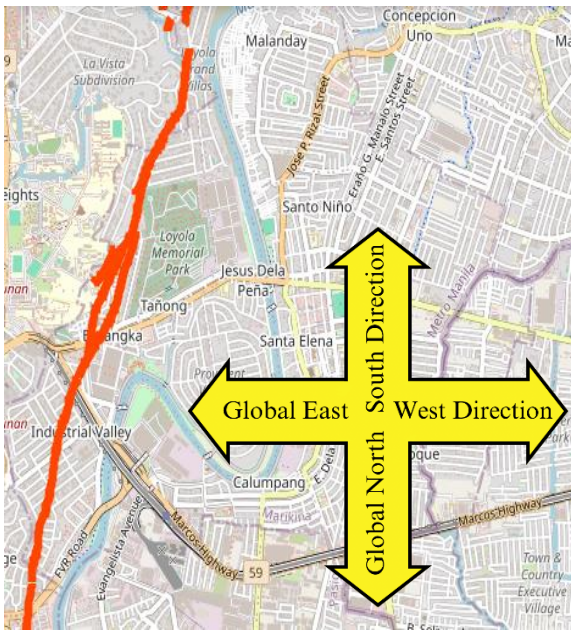

Fig. 1 Map of West Valley Fault including Marikina City with the orientation of the global east-west direction and global north-south direction

This study aims to predict the structural damage to six existing reinforced concrete structures from a two-kilometer distance from the West Valley Fault through a fragility curve once the anticipated 7.2 magnitude earthquake, or the so-called "Big One," hits Marikina City.

The prediction of seismic damage was limited to six structures, ranging from low-rise to mid-rise, with varying occupancy types due to a lack of accessible high-rise structures within a two-kilometer range from the West Valley Fault in Marikina City. Moreover, this study limits the prediction of seismic damage on reinforced concrete structures within the superstructure, exclusive of the effects of soil liquefaction and the settlement of the foundation.

The modeled reinforced concrete structures with varying story levels and occupancy types were rotated based on their actual configuration with respect to the West Valley Fault, as shown in Fig. 2.

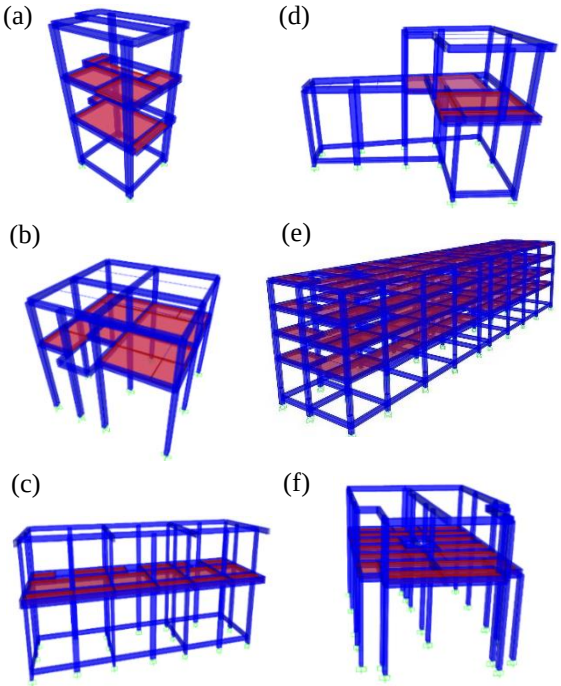

Fig. 2 Modeled reinforced concrete structures (a) Structure A (b) Structure B (c) Structure C (d) Structure D (e) Structure E (f) Structure F

2. RESEARCH SIGNIFICANCE

The last time the West Valley Fault generated seismic motion was during the 17th century, and its projected return period is 500 years, which approximately coincides with today's time. The conclusions and recommendations made in this research could be used to implement damage mitigation policies and increase public awareness regarding the "Big One." It may also serve as a reference for the design and construction of structures in areas within a two-kilometer range from the West Valley Fault and the rehabilitation of existing structures constructed before the current structural code was conceptualized.

3. METHODS

3.1 Modeling of the Structures

The authors requested the structural and architectural plans of reinforced concrete structures within a two-kilometer distance from the fault line in Marikina City from the building owners.

The West Valley Fault Proximity Map through the ArcGIS application provided access to the scaled map of Marikina City, which also shows the West Valley Fault's configuration. The West Valley Fault

Proximity Map could measure how far the analyzed structure is to the fault line. The structures are rotated to represent their actual configuration in order to simulate their actual seismic response. The reinforced concrete frame, including the tie-beam, if there were any, was modeled through SAP2000, a structural engineering software.

The dimensions of each structural member and their associated properties, such as yield strength and concrete compressive strength, were based on the obtained structural plans. Likewise, the structural model included the spacing of the transverse reinforcements and the quantity and orientation of the embedded longitudinal bars as per the structural plans.

Referencing Mariano and Estores [9], for the simplicity of the analysis, a fixed support condition was used in the isolated footings for all analyzed structures.

3.1.1 Assignment of Gravity Loads

The basis for the superimposed dead loads in the modeled structure is the architectural plans. It indicates the divisions per floor, the use or occupancy of each room, the materials used for the floor finishes and partitions, and the thickness of the masonry walls. On the other hand, the values for the live loads depend on the occupancy or use of each room, which has a corresponding value in the NSCP 2015.

The values for both superimposed dead and live loads were obtained from NSCP 2015, which served as the gravity loads in the simulation. SAP2000 automatically calculated the self-weight of all the structural members.

3.1.2 Assignment of Seismic Loads

The values to determine seismic loads in the structures depend on the structure period, overstrength factor, seismic source type, soil profile type, near-source factors, and seismic importance factor, whose values can be found in the Uniform Building Code [10].

The constant value Ct, used to calculate the structure period for reinforced concrete moment-resisting frames, is fixed at 0.0731. Since Marikina City is under Seismic Zone 4, the seismic zone factor for all analyzed structures is 0.4. Likewise, for reinforced concrete structures under Zone 4, the overstrength factor is 8.5.

Seismic Source Type A is used for all the structures since this source type can generate a range of 7.0 to 8.4 magnitude, in which the predicted 7.2 magnitude earthquake falls within this range. For the near-source factors for structures under Seismic Source Type A, the values for N_a and N_v are 1.50 and 2.00, respectively. Seismic coefficients, C_a and C_v, depend on the seismic zone and the soil profile type.

The soil profile types are characterized by their shear wave velocity. Soil profile types are determined through the study of Dungca et al. [11], which shows the soil-bearing capacity of Marikina City, followed up by the work of Tezcan and Ozdemir [12], which correlates the relationship between soil-bearing capacity and shear wave velocity.

The seismic importance factor depends on the occupancy category. The different occupancy categories are defined as essential facilities, hazardous facilities, special occupancy structures, standard occupancy structures, and miscellaneous structures, with a Seismic Importance Factor of 1.50, 1.25, 1.00, 1.00, and 1.00, respectively.

3.2 Nonlinear Static Pushover Analysis

Given the necessary parameters, nonlinear static pushover analysis was performed through SAP2000. The assigned mass source for the structure is all the gravity loads present, including the self-weight of the structural members. A nonlinear gravity load case was then applied, with its initial condition starting from an unstressed state.

Due to the unpredictability of the earthquake motion, nonlinear static pushover analysis was performed and analyzed separately for the global east-west direction and the global north-south direction.

The static nonlinear pushover analysis for both seismic directions continue from the state at the end of the nonlinear gravity load case. A control node is assigned at the topmost level of each analyzed structure. The designated control node per structure is the same for the mass source, nonlinear gravity load case, and nonlinear static pushover analysis in both seismic directions.

3.2.1 Pushover Hinges

The parameters for the pushover hinges are based on the provisions provided by the Structural Engineering Institute [13] for both rectangular or square concrete columns and concrete beams. The pushover hinges are assigned at the 5% mark of the total length of the beams and columns originating from the beam-column joint. According to Talantova [14], the most critical element that affects a reinforced concrete structure during earthquakes is the joint where the beams and columns intersect.

3.2.2 Idealized Force-Displacement Curve

Based on FEMA 356 [15], the idealized force-displacement curve is automatically generated in SAP 2000 once a nonlinear static pushover analysis is executed. The resulting curves determine the values for the control node's yield displacement, Δy, and target displacement, Δt. It is comprised of two-line segments, each corresponding to the structure's stiffness. The corresponding roof displacement on the point terminating the initial stiffness is the yield displacement, while the corresponding roof displacement on the point terminating the final

stiffness is the target displacement.

3.3 Determining the Damage States

Table 1 tabulates the four structural damage states that are qualitatively defined in the HAZUS MH 2.1 Technical Manual [16] for reinforced concrete moment-resisting frames

Table 1. Qualitative description of structural damage states

Damage State	Description
Slight Damage State	Flexural or shear-type hairline cracks within the beam-column joint.
Moderate Damage State	Hairline cracks in columns and beams. Yield capacity occurs, evidenced by concrete spalling and flexural cracks. Shear cracks are more evident, and spalling may occur for nonductile frames.
Severe Damage State	Ultimate capacity occurs, evidenced by buckling, concrete spalling, and noticeable flexural cracks. Partial collapse may already happen in nonductile frames.
Complete Damage State	The structure is at risk of collapse due to the loss of frame stability and brittle failure of nonductile frames.

The four damage states are correlated quantitatively with the yield spectral displacements and target spectral displacements obtained through the capacity spectrum conversion.

3.3.1 Capacity Spectrum Conversion

The yield displacement and target displacement obtained from the idealized force-displacement curve are converted to yield spectral displacement, D_y, and target spectral displacement, D_u, under the capacity spectrum conversion prescribed in ATC 40 [17]. Two sets of D_y and D_u were produced: one for the global east-west direction and one for the global north-south direction.

Eq. (1) converts yield displacement, Δy, into yield spectral displacement, D_y. On the other hand, Eq. (2) is the conversion of target displacement, Δt, into target spectral displacement, D_u.

$$D_y = \frac{\Delta y}{PF_1 \emptyset_{roof,1}} \quad (1)$$

$$D_u = \frac{\Delta t}{PF_1 \emptyset_{roof,1}} \quad (2)$$

PF_1 is defined as the modal participation factor for the first mode, while $\emptyset_{roof,1}$ denotes the amplitude of the first mode of the control node. Both values are calculated in SAP 2000.

3.3.2 Correlation between spectral displacement and damage states

The correlation between the damage states and the spectral displacement has been established by Barbat et al. [18]. The spectral displacement of the control node at which the likelihood of a particular damage state exceeding 50% is shown in Eq. (3) to Eq. (6).

When the control node reaches a displacement at a specific seismic direction, as indicated in Eq. (3), there is a likelihood of 50% that the structure will experience structural damage beyond the slight damage state.

$$D_{50\%\, slight} = 0.7 D_y \quad (3)$$

At a particular seismic direction, once the control node experienced a displacement the same as the yield spectral displacement, as shown in Eq. (4), there is a likelihood of 50% that the structure will experience structural damage beyond the moderate damage state.

$$D_{50\%\, moderate} = D_y \quad (4)$$

Structural damage exceeding the severe state will have a 50% chance of occurring when the control node undergoes a displacement, as indicated in Eq. (5).

$$D_{50\%\, severe} = D_y + 0.25\left(D_u - D_y\right) \quad (5)$$

Finally, there is a 50% possibility that the structure will completely collapse when the control node matches the value of the target spectral displacement, as shown in Eq. (6).

$$D_{50\%\, complete} = D_u \quad (6)$$

3.4 Plotting of Fragility Curves

The fragility curves for each structure are formulated separately for the two seismic directions in anticipation of the possible motion of the 7.2 magnitude earthquake. The probability of exceedance, plotted in the vertical axis, is defined as the probability at which the structural damage state at any given intensity measure exceeds the effects of that particular damage state. In contrast, the intensity measure, the spectral displacement, is plotted on the horizontal axis.

The fragility curve of a single structure has four curves, each representing the four structural damage states. Eq. (7) calculates the probability of exceedance of a specific damage state. Eq. (7) is performed four times in a single fragility curve to

represent the four damage states.

$$P_f(DS > ds_i \mid S_D) = \Phi\left[\frac{1}{\beta} ln\left(\frac{S_D}{D_{50\%}}\right)\right] \quad (7)$$

The standard normal cumulative distribution function is denoted by the variable Φ. $D_{50\%}$ corresponds to the value of $D_{50\%\, slight}$ for slight damage, $D_{50\%\, moderate}$ for moderate damage, $D_{50\%\, severe}$ for severe damage and $D_{50\%\, \text{complete}}$ for complete damage state.

β is calculated by first forming a set of data points, S_D, in MATLAB. These data points are the spectral displacements assigned at a specific interval, starting from a value lower than Δ_y until a value higher than D_u. The interval for those data points can be adjusted as long as the value of $D_{50\%}$ is included, and the resulting fragility curve fits and is enough to be interpreted. β is then calculated as the standard deviation of the natural logarithm of each data point.

3.5 Damage Prediction

The probability of exceedance in the fragility curve is identified through the maximum displacement of the control node due to the ultimate load combination, Δ_{max}, per seismic direction.

Δ_{max} is plotted in the horizontal axis of each fragility curve per direction, then projected to its corresponding exceedance probability for every damage state in the vertical axis. The eight ultimate load combinations based on NSCP 2015 are shown in Eq. (8) to Eq. (15).

$$1.3DL + LL + S_{EW} \quad (8)$$

$$1.3DL + LL - S_{EW} \quad (9)$$

$$1.3DL + LL + S_{NS} \quad (10)$$

$$1.3DL + LL - S_{NS} \quad (11)$$

$$0.8DL + S_{EW} \quad (12)$$

$$0.8DL - S_{EW} \quad (13)$$

$$0.8DL + S_{NS} \quad (14)$$

$$0.8DL - S_{NS} \quad (15)$$

DL denotes the dead loads, LL corresponds to the live loads, S_{EW} represents the seismic load in the east-west direction, while S_{NS} represents the seismic load in the north-south direction.

3.6 Statistical Analysis Test

T-tests with independent samples were performed on each of the four damage states through Statistical Package for the Social Sciences (SPSS). The means of each structure's probability of exceedance in a specific damage state in the global east-west direction is compared to the probability of exceedance in a specific damage state in the north-south direction with a significance level of 0.05.

4. RESULTS AND DISCUSSION

4.1 Generated Fragility Curves

Table 2 tabulates each structure's control node magnitude and the ultimate load combination that yielded the maximum displacement for the two seismic directions. The resulting fragility curves per structure were verified by examining the coordinates of the values for $D_{50\%slight}$, $D_{50\%moderate}$, $D_{50\%severe}$, and $D_{50\%complete}$ in the horizontal axis. The generated curves show consistency in that the values for $D_{50\%}$ for both seismic directions are shown to have exactly a 50% probability of exceeding their respective structural damage states.

Table 2. Magnitude of each structure's control node

	PF_1	$\emptyset_{roof,1}$	$D_{50\%\, slight}$	$D_{50\%\, moderate}$	$D_{50\%\, severe}$	$D_{50\%\, complete}$	Δ_{max}	Governing Load Combination
	Global East-West Direction							
Structure A	6.86	0.0814	0.0363m	0.0519m	0.0855m	0.1862m	0.0442m	Eq. (8)
Structure B	10.01	0.1067	0.0191m	0.0273m	0.0490m	0.1142m	0.0269m	Eq. (9)
Structure C	15.41	0.0624	0.0138m	0.0197m	0.0418m	0.1081m	0.0226m	Eq. (9)
Structure D	8.01	0.1836	0.0071m	0.0102m	0.0325m	0.0992m	0.0251m	Eq. (9)
Structure E	7.74	0.03	0.1134m	0.1620m	0.3057m	0.7367m	0.0403m	Eq. (9)
Structure F	12.17	0.09	0.0083m	0.0119m	0.024m	0.0603m	0.027m	Eq. (9)
	Global North-South Direction							
Structure A	7.7	0.0933	0.0283m	0.0404m	0.1009m	0.2826m	0.0394m	Eq. (10)
Structure B	2.72	0.0352	0.1667m	0.2382m	0.2935m	0.4596m	0.0157m	Eq. (15)
Structure C	6.53	0.0352	0.0518m	0.0740m	0.1176m	0.2482m	0.0187m	Eq. (11)
Structure D	1.19	0.0392	0.1945m	0.2779m	0.8069m	2.39m	0.0189m	Eq. (11)
Structure E	50.31	0.0124	0.0229m	0.0327m	0.1267m	0.4087m	0.0467m	Eq. (11)
Structure F	4.58	0.0273	0.0126m	0.0179m	0.0475m	0.1361m	0.0138m	Eq. (11)

4.1.1 Fragility Curves for Structure A

Structure A is a 3-story residential structure in Barangay Tumana, 813 meters from the West Valley Fault. Its fragility curves and corresponding Δ_{max} value for both seismic directions are projected to its corresponding probability of exceedance per damage state, as shown in Fig. 3.

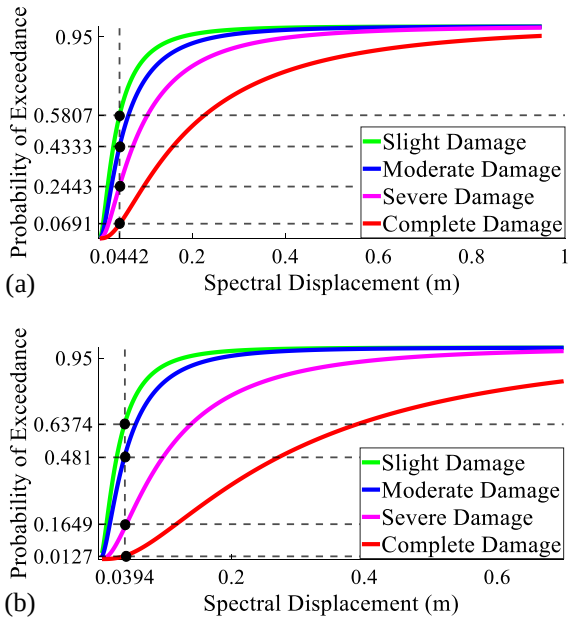

Fig 3. Fragility curves for Structure A (a) global east-west direction (b) global north-south direction

4.1.2 Fragility Curves for Structure B

Structure B is a 2-story commercial building whose occupants are different offices and food stalls. This structure is in Barangay Nangka, 770 meters from the West Valley Fault.

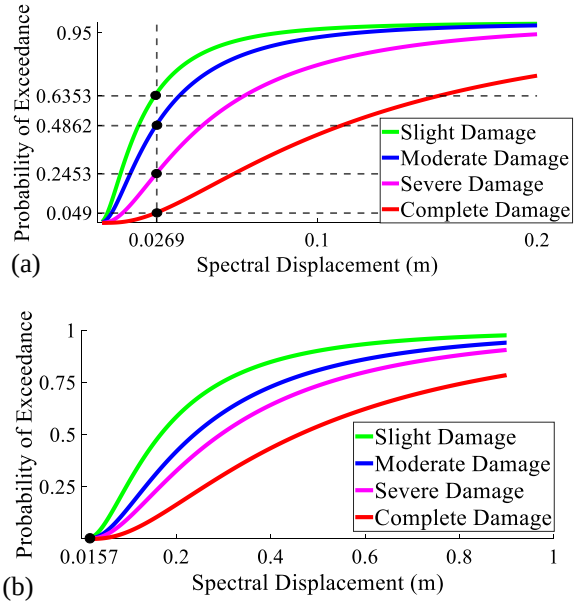

Fig 4. Fragility curves for Structure B (a) global east-west direction (b) global north-south direction

According to its fragility curve in Fig. 4, there is no chance for the structure to exceed a slight structural damage state in the global north-south direction; thus, there will be no structural damage to the structure when the control node displaces a magnitude of Δ_{max} in the global north-south direction.

4.1.3 Fragility Curves for Structure C

Structure C is a 2-story residential apartment building in Barangay Nangka, 895 meters from the West Valley Fault. Its fragility curves and corresponding Δ_{max} value for both seismic directions, projected to its corresponding probability of exceedance per damage state, are shown in Fig. 5.

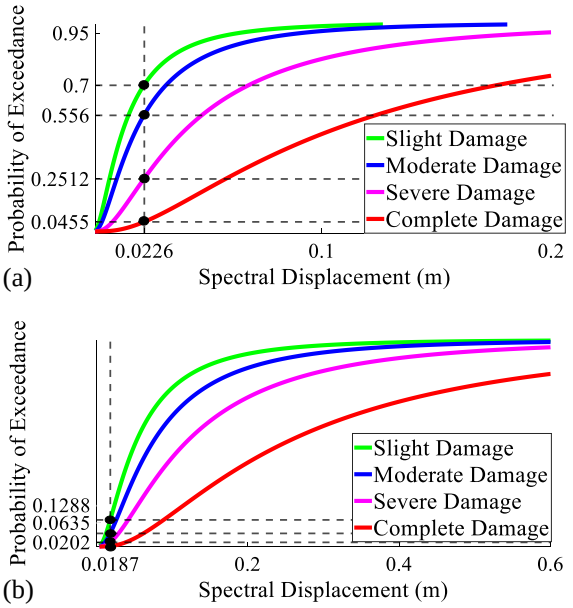

Fig 5. Fragility curves for Structure C (a) global east-west direction (b) global north-south direction

4.1.4 Fragility Curves for Structure D

Structure D is a 2-story multipurpose private resort building located in Barangay Calumpang, 1.43 kilometers from the West Valley Fault.

The fragility curve in Fig. 6 indicates that there is no chance for the structure to exceed a slight structural damage state in the global north-south direction; thus, there will be no structural damage to the structure when the control node displaces a magnitude of Δ_{max} in the global north-south direction.

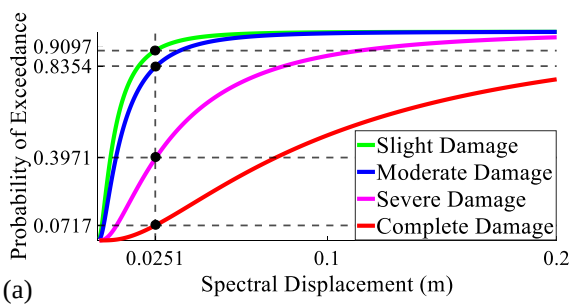

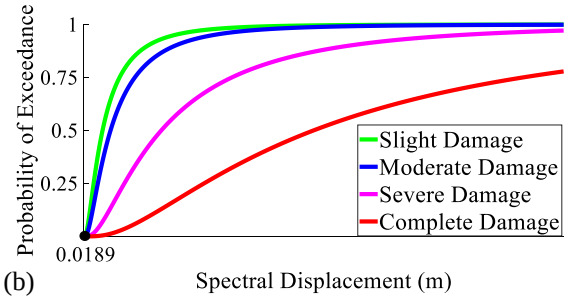

Fig 6. Fragility curves for Structure D (a) global east-west direction (b) global north-south direction

4.1.5 Fragility Curves for Structure E

Structure E is a school building in Barangay Sta Elena, 1.75 kilometers from the West Valley Fault. It has a total of 4-stories for academic purposes and a roof deck for recreational use.

As illustrated in its fragility curves in Fig. 7, there is no chance for the structure to exceed a slight structural damage state in the global east-west direction; thus, it follows that there will be no structural damage to the structure when the control node displaces a magnitude of Δmax in the global east-west direction.

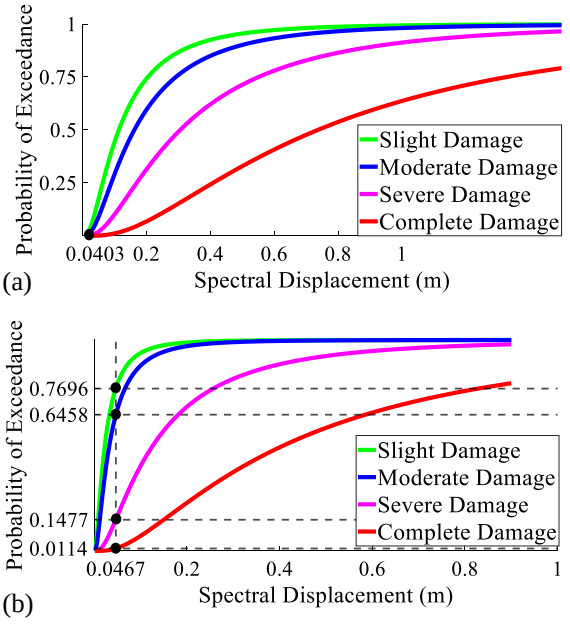

Fig 7. Fragility curves for Structure E (a) global east-west direction (b) global north-south direction

4.1.6 Fragility Curves for Structure F

Structure F is a 2-story residential structure located in Barangay Sta Elena, 1.73 kilometers from the fault line. Fig. 8 illustrates the fragility curves for Structure F. The corresponding values for Δmax for the global east-west and north-south directions are projected to their corresponding exceedance probability.

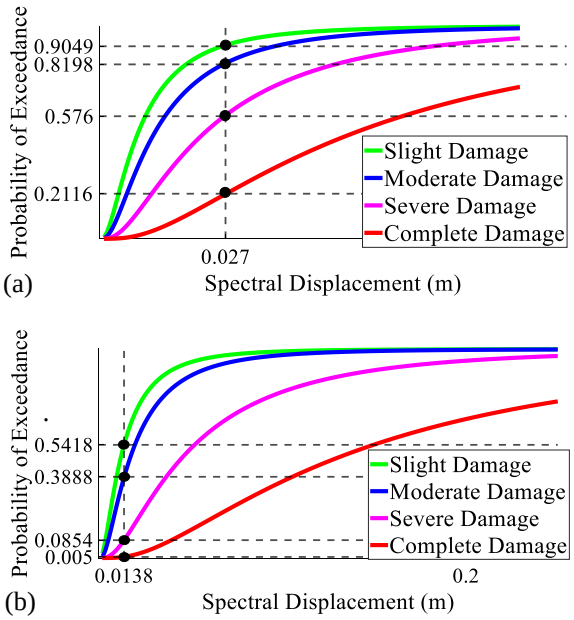

Fig 8. Fragility curves for Structure F (a) global east-west direction (b) global north-south direction

4.2 Statistical Analysis Test Results

Based on the generated fragility curves, the probability of exceeding a particular damage state for the two seismic directions across the six structures is tabulated in Tables 3 to 6. Moreover, since the mean values for the global east-west and north-south direction across all the six analyzed structures were being compared to each other in a particular structural damage state in the independent samples t-test, the tables include the mean values for the global east-west and north-south directions, along with the resulting p-value from the independent samples t-test.

Table 3. Structures' probability of exceeding the slight damage state for the two seismic directions, including the resulting mean and p-values

	Global East-West Direction	Global North-South Direction	P-value
Structure A	58.07%	63.74%	0.189
Structure B	63.53%	0%	
Structure C	70%	12.88%	
Structure D	90.97%	0%	
Structure E	0%	76.96%	
Structure F	90.49%	54.18%	
Mean Value	62.18%	34.63%	

As tabulated in Table 3, the mean for the probability of exceedance of the structures in the slight damage state in the global east-west direction is 62.18%, which is higher than the mean for the global north-south direction, which is 34.63%. Still, the means of the two have no significant difference since the resulting p-value for the t-test in the slight damage state is 0.189, which is higher than the significance level of 0.05.

Table 4. Structures' probability of exceeding the moderate damage state for the two seismic directions, including the resulting mean and p-values

	Global East-West Direction	Global North-South Direction	P-value
Structure A	43.33%	48.10%	0.157
Structure B	48.62%	0%	
Structure C	55.60%	6.35%	
Structure D	83.54%	0%	
Structure E	0%	64.58%	
Structure F	81.98%	38.88%	
Mean Value	52.18%	26.32%	

As tabulated in Table 4, it shows that the mean for the probability of exceedance of the structures in the moderate damage state in the global east-west direction is 52.18%, which is higher than the mean for the global north-south direction, which is 26.32%. The resulting p-value for the t-test in the moderate damage state is 0.157, greater than the significance level of 0.05. It implies that the means of the two seismic directions in the moderate damage state are not significantly different.

Table 5. Structures' probability of exceeding the severe damage state for the two seismic directions, including the resulting mean and p-values

	Global East-West Direction	Global North-South Direction	P-value
Structure A	24.43%	16.49%	0.027
Structure B	24.53%	0%	
Structure C	25.12%	2.02%	
Structure D	39.71%	0%	
Structure E	0%	14.77%	
Structure F	57.60%	8.54%	
Mean Value	28.56%	6.97%	

Table 5 tabulates the means for the probability of exceedance of the structures in the severe damage state for the two seismic directions. The mean for the global east-west direction is higher than that for the global north-south direction, with values of 28.56% and 6.97%, respectively. The p-value for the t-test in the severe damage state is 0.027, which is less than the significance level of 0.05. This indicates a significant difference between the means of the two seismic directions for the severe damage state.

Table 6. Structures' probability of exceeding the complete damage state for the two seismic directions, including the resulting mean and p-values

	Global East-West Direction	Global North-South Direction	P-value
Structure A	6.91%	1.27%	0.041
Structure B	4.90%	0%	
Structure C	4.55%	0.21%	
Structure D	7.17%	0%	
Structure E	0%	1.14%	
Structure F	21.16%	0.50%	
Mean Value	7.45%	0.52%	

Lastly, the probability of exceedance of the structures in the complete damage state for the two seismic directions is tabulated in Table 6. It again indicates that the mean for the global east-west direction is higher than that of the global north-south direction, with values of 7.45% and 0.52%, respectively. There is a significant difference between the two seismic directions in the complete damage state due to the p-value being 0.041, which is less than the significance level of 0.05.

4.3 Interpretation of the Fragility Curves

In the generated fragility curves, the values for $D_{50\%slight}$ are shown to have exactly a probability of 50% exceeding slight damage. $D_{50\%moderate}$ value has exactly a 50% chance of surpassing moderate damage, $D_{50\%severe}$ was found to have exactly a likelihood of 50% to go beyond severe damage, and lastly, the value of $D_{50\%complete}$ indicates precisely a 50% probability of complete collapse, which validated the generated fragility curve as a reliable tool for further seismic damage prediction to structures. Likewise, the results showed consistency; as the values for $D_{50\%}$ increased, the structure's probability of sustaining structural damage decreased.

The varying damage severity due to the structure's configuration complements the field assessment of Ismail et al. [19] in structures after the earthquake in 2009 and 2018. From the data gathered on the damaged structure after the 2009 earthquake in Padang, an observation was made that the severity of the structural damages in its columns varies depending on its position within the structure. A similar observation from the 2009 earthquake is documented in a different structure in the aftermath of the 2018 Palu earthquake, wherein some columns suffered severe damage while others were said to be in decent condition.

Likewise, the varying damage severity due to seismic motion is validated by the independent samples t-test, which indicates that the mean of the effects of the seismic motion in the global east-west and north-south directions for the severe damage state and the complete damage state are significantly different.

A common characteristic has been established for structures with no probability of structural damage in a specific direction; these structures complied with the minimum column dimension for special moment frames, 300mm. The result of this study suggesting that a structure may not even experience any structural damage despite being subjected to a 7.2 magnitude earthquake is validated through the field observations made by Putra [20] in the aftermath of the 7.9 magnitude Bengkulu earthquake in 2007 and the 7.6 magnitude Padang earthquake in 2009. In the aftermath of the 7.9 magnitude earthquake in Padang

City, an observation was made in a specific structure that only its non-structural members were destroyed. In a different structure, two years later, a 7.6 magnitude earthquake hit Padang City; only the non-structural members experienced heavy damage, while the damage to its structural members was considered minimal.

Out of the six analyzed structures, only Structure E is predicted not to suffer from any structural damages when the anticipated 7.2 magnitude earthquake moves in the global east-west seismic direction. However, it is the critical direction for Structures A, B, C, D, and F. If the anticipated 7.2 magnitude earthquake were to move in the global east-west seismic direction, those structures would likely sustain flexural or shear-type hairline cracks within their beam-column joints, which corresponds to slight structural damage. However, there is a considerable possibility of severe structural damage to these structures that would manifest column buckling, obvious flexural cracks, and concrete spalling to the structural members. A complete collapse for the mentioned structures in the global east-west direction seemed unlikely except for Structure F, whose fragility curve indicates a 21.16% chance of being subjected to complete damage.

Only Structures A, C, and F have a probability of experiencing structural damage if the seismic motion moves in either the global east-west or north-south directions. Structure A and Structure C have a minimum column dimension of 250mm, while Structure F has a minimum column dimension of just 200mm. The minimum column dimension requirement for special moment frames is 300mm. These three structures are the only ones non-compliant with the minimum column dimension for special moment frames, especially Structure F, whose column dimension is way below the minimum required. This circumstance would justify the results that Structure F has the highest probability of collapsing.

A correlation between the column dimension and the probability of structural damage in a structure is validated through the findings of Fauzan et al. [21], who also developed seismic fragility curves for a four-story reinforced concrete school building in Padang, Indonesia. Their study compared the damage states of the existing structure and whether the structural columns of the four-story school building were to be retrofitted through concrete jacketing, which would increase the cross-sectional area of the columns. Their study concluded that the probability of exceeding the extensive damage state decreased by 42.06%, and the probability the structure would collapse decreased by 4.42% if its column dimensions were to be increased through concrete jacketing, which implies that increasing the column dimensions would reduce the severity of the structural damage state.

5. CONCLUSION

Multiple literature reviews suggest predicting seismic damage through a lognormal cumulative distribution function-defined fragility curve. Two fragility curves per structure were analyzed separately due to the unpredictable nature of the seismic motion, one for the global east-west direction and the other for the global north-south direction.

Structures that are concluded not to sustain structural damage in a specific seismic direction are still prone to non-structural damage, such as the collapse of ceilings, wall partitions, glass walls, brick or hollow block walls, and falling pieces of furniture that may still disrupt operations, cause economic repercussions, injuries or fatalities.

For any proposed structures to be built in Marikina City, their configuration with respect to the West Valley Fault should be incorporated into the structural design since the severity of the structural damage varies depending on its configuration.

The resulting fragility curves suggest a higher probability of structural damage for existing structures whose column dimensions are less than the prescribed dimension for special moment resisting frames. Likewise, structural engineers should be firm in incorporating a special moment resisting frame for their structural designs, especially the dimensional limits of every structural member, and ensure that the design is being implemented and monitored during the construction phase for areas under Zone 4 and within a two-kilometer range from a known seismic source.

Future researchers could reference the results of this study to determine an efficient retrofitting method to decrease the possibility of severe damage or collapse to the structures if the motion of the anticipated 7.2 magnitude earthquake is in the structure's critical direction. To further bridge the gap in conducting seismic damage predictions on reinforced concrete structures, future studies are recommended to conduct the study in an area more than two kilometers from the West Valley Fault with a high concentration of high-rise structures and include the effects of soil liquefaction and the settlement of the foundation.

6. ACKNOWLEDGMENTS

The authors would like to acknowledge and express their deepest gratitude to Engr. Wyndell A. Almenor, Engr. Rolando J. Quitalig, and Engr. Charity Hope A. Gayatin, for their guidance and recommendations during the research.

7. REFERENCES

[1] JICA., MMDA., and PHIVOLCS., Final Report Volume 1: Executive Summary Earthquake

Impact Reduction Study for Metropolitan Manila, Republic of the Philippines. NDRRMC, 2004, pp. 11-13.

[2] Association of Structural Engineers of the Philippines., Minimum Design Loads, National Structural Code of the Philippines Volume 1: Buildings, Towers, And Other Vertical Structures, ASEP, 2015, Quezon City, Philippines, pp. 11-236.

[3] American Committee 318., Earthquake Resistance, Building Code Requirements for Structural Concrete (ACI318M-14) and Commentary (ACI318RM-14). American Concrete Institute, 2014, Farmington Hills, Michigan, pp. 263-312.

[4] Karimzadeh S., Miyajima M., Hassanzadeh R., Amiraslanzadeh R. and Kamel B., A GIS-based seismic hazard, building vulnerability and human loss assessment for the earthquake scenario in Tabriz. Soil Dynamics and Earthquake Engineering, Vol. 66, 2014, pp. 263–280.

[5] Alothman A., Mangalathu S., Al-Mosawe A., Alam M.M. and Allawi A., The influence of earthquake characteristics on the seismic performance of reinforced concrete buildings in Australia with varying heights. Journal of Building Engineering, Vol. 67, 2023, pp. 105957.

[6] Ghani K.D.A., Sakdun N.S.M., Kusumawardani R., Hamed A.F.A. and Roslan M.A.H., Seismic Assessment of Multi-Storey Residential Building using Fragility Curve and Capacity Demand Response Spectrum. AIP Conf Proc, Vol. 2532, No.1, 2022, pp.040008.

[7] Vasileiadis V., Kostinakis K., and Athanatopoulou A., Story-wise assessment of seismic behavior and fragility analysis of R/C frames considering the effect of masonry infills. Soil Dynamics and Earthquake Engineering, Vol. 165, 2023, pp. 107714.

[8] Gentile R., Galasso C., Idris Y., Rusydy I. and Meilianda E., From rapid visual survey to multi-hazard risk prioritization and numerical fragility of school buildings. Natural Hazards and Earth System Sciences, Vol. 19, No. 7, 2019, pp. 1365–1386.

[9] Mariano J. and Estores G., Seismic Response Analysis of Bongo Bridge Subjected to Multiple Support Excitation due to Spatial Variation of Ground Motion. Civil Engineering and Architecture, Vol. 10, No. 4, 2022, pp. 1405-1418.

[10] Uniform Building Code (UBC-97)., Structural Design Requirements, International Conference of Building Officials, 1997, Whittier, California, pp. 9-35.

[11] Dungca J.R., Concepcion I., Limyuen M.C.M., See T.O. and Vicencio M.R., Soil bearing capacity reference for Metro Manila, Philippines. International Journal of GEOMATE, Vol. 12, No. 32, 2017, pp. 5–11.

[12] Tezcan S. and Ozdemir Z., A Refined Formula for the Allowable Soil Pressure Using Shear Wave Velocities. Journal of Civil Engineering and Architecture, vol. 6, 2012, pp. 470–478.

[13] Structural Engineering Institute., Concrete, Seismic Evaluation and Retrofit of Existing Buildings. ASCE, 2017, Reston, Virginia, pp.150-152.

[14] Talantova K.V., Computer-aided design of civil building structural connections constructed in earthquake-prone regions. IOP Conference Series: Materials Science and Engineering, Vol. 9, 2018, pp.012028.

[15] Federal Emergency Management Agency., Analysis Procedure, FEMA 356 Prestandard and Commentary for Seismic Rehabilitation of Buildings. FEMA, 2000, Washington DC, USA, pp. 19-24.

[16] Federal Emergency Management Agency Earthquake Committee., Direct Physical Damage-General Building Stock, Multi-hazard Loss Estimation Methodology Earthquake Model HAZUS-MH 2.1 Technical Manual. FEMA, 2012, Washington DC, USA, pp.20.

[17] Applied Technology Council., Retrofit Strategies ATC-40 Seismic Evaluation and Retrofit of Concrete Buildings: Volume 1. ATC, 1996, California, USA, pp. 7-10.

[18] Barbat A.H., Pujades L.G. and Lantada N., Seismic damage evaluation in urban areas using the capacity spectrum method: Application to Barcelona. Soil Dynamics and Earthquake Engineering, Vol. 28, No. 10–11, 2008, pp. 851–865.

[19] Ismail F., Hakam A., Putra H., Hape M.M. and Asmirza M.S., Comparison study on damage pattern of two stories building: simulation vs field record. International Journal of GEOMATE, Vol. 18, No. 70, 2020, pp. 37-42.

[20] Putra R., Damage investigation and re-analysis of damaged building affected by the ground motion of the 2009 Padang Earthquake. International Journal of GEOMATE, Vol. 18, No. 66, 2020, pp. 163–170.

[21] Fauzan., Kurniawan R., Syahdiza N., Al Jauhari Z. and Nugraha M.D.A., Fragility Curve of School Building in Padang City With and Without Retrofitting Due To Earthquake and Tsunami Loads. International Journal of GEOMATE, Vol. 24, No. 101, 2023, pp. 102–109.